Journal of Solid State Chemistry **156,** 331–338 (2001)
doi:10.1006/jssc.2000.9003, available online at http://www.idealibrary.com on IDEAL®

Synthesis of $Na_xMnO_{2+\delta}$ by a Reduction of Aqueous Sodium Permanganate with Sodium Iodide

Y. U. Jeong and A. Manthiram[1]

Texas Materials Institute, ETC 9.104 The University of Texas at Austin Austin, Texas 78712

Received March 20, 2000; in revised form October 5, 2000; accepted October 13, 2000; published online December 21, 2000

Reduction of sodium permanganate with sodium iodide in aqueous solutions has been investigated systematically. The products formed have been characterized by X-ray diffraction, wet-chemical analysis, and surface area and magnetic susceptibility measurements after firing at various temperatures. The results reveal that the sodium content x in the reduction products $Na_xMnO_{2+\delta}$ depends strongly on the reaction pH and mildly on the relative concentrations of the reactants. $Na_{0.7}MnO_{2+\delta}$ obtained at pH > 11 followed by firing at $T > 500^\circ C$ adopts the $P2$ layer structure (hexagonal) with cation vacancies arising from a $\delta \approx 0.3$. $Na_{0.7}MnO_{2+\delta}$ crystallizing in a distorted $P2$ structure (orthorhombic) without cation vacancies ($\delta \approx 0$) could be obtained by annealing the hexagonal $Na_{0.7}MnO_{2+\delta}$ ($\delta \approx 0.3$) in N_2 atmosphere around 600°C. While the orthorhombic $Na_{0.7}MnO_{2+\delta}$ ($\delta < 0.05$) is stable during ion-exchange reactions with lithium salts at $25 \le T \le 180^\circ C$, the hexagonal $Na_{0.7}MnO_{2+\delta}$ ($\delta \approx 0.3$) transforms to spinel-like phases due to the presence of cation vacancies. $Na_{0.5}MnO_{2+\delta}$ obtained at a controlled pH of 9.3 adopts a metastable layer structure on firing at 500°C and a tunnel structure isostructural with $Na_4Mn_4Ti_5O_{18}$ on firing at $T \ge 600^\circ C$. The tunnel structure is stable to ion-exchange reactions without transforming to spinel-like phases. In addition, washing the reduction products with various organic solvents before firing at higher temperatures is found to influence the reaction kinetics, composition, and crystal chemistry. © 2001 Academic Press

1. INTRODUCTION

Manganese oxides exhibit a rich variety of crystal chemistry (1, 2) and physical properties including the recently discovered colossal magnetoresistance (3). Binary and ternary manganese oxides find several applications such as electrode materials in primary and secondary batteries (4), mixed ionic–electronic conductors in solid oxide fuel cells (5), and catalysts (6). The exponential growth in portable electronic devices such as cellular phones and laptop computers has created enormous interest in lightweight batteries such as the lithium-ion batteries. In a drive to develop relatively inexpensive and environmentally benign electrode materials for lithium-ion batteries, manganese oxides have drawn much attention. The interest in manganese oxides as electrode hosts has created intensive worldwide activity on the synthesis and characterization of manganese oxides particularly by low-temperature, soft chemistry procedures (1, 7).

Sodium manganese oxides $Na_xMnO_{2+\delta}$ ($0 \le x \le 1$) form several phases with allotropic modifications depending on the values of x and δ (8, 9). Some examples are $Na_{0.2}MnO_2$, $Na_{0.4}MnO_2$, $Na_{0.44}MnO_2$, $Na_{0.7}MnO_{2+\delta}$ ($0 \le \delta \le 0.25$), and $NaMnO_2$. Sodium manganese oxides have been synthesized both by conventional solid-state reactions (8–11) between sodium salts and manganese oxides or salts as well as by soft chemistry synthesis procedures (12–15). For example, they have been synthesized by a sol–gel reaction between $NaMnO_4$ and glucose (12), reaction between $MnCl_2$ and NaOH solutions followed by heating the suspension at 85°C (13), reaction between $NaMnO_4$ and Mn^{2+} under alkaline conditions (14), and hydrothermal treatment of γ-MnO_2 with NaOH solution in an autoclave (15).

We present in this paper the synthesis of $Na_xMnO_{2+\delta}$ by reducing sodium permanganate by sodium iodide in aqueous solutions. The influence of the reduction reaction pH, concentration of reactants, washing agents, and post-heat-treatment temperature on the crystal chemistry and composition of the products is presented. The procedure gives layered $Na_{0.7}MnO_{2+\delta}$ ($0 \le \delta \le 0.3$) and layered and tunnel $Na_{0.5}MnO_{2+\delta}$ ($0 \le \delta \le 0.15$). The structural stability of the phases during ion exchange with lithium salts to obtain cathode materials for lithium cells is presented. In addition, the magnetic properties of the $Na_xMnO_{2+\delta}$ phases are presented.

2. EXPERIMENTAL

The reduction of sodium permanganate with sodium iodide was performed by two procedures. In the first procedure, 100 mL of 0.5 M aqueous solution of $NaMnO_4 \cdot H_2O$ was

[1] To whom correspondence should be addressed.

0022-4596/01 $35.00

mixed with 100 mL of various concentrations (0.05–3 M) of aqueous NaI and stirred for 24 h on a magnetic stirrer; this procedure is designated as "reduction reactions without pH control." In the second procedure, 50 mL of 0.1 or 0.5 M aqueous solution of NaI was added slowly from a burette into 50 mL of aqueous solution of 0.1 or 0.5 M $NaMnO_4$ that was kept under constant stirring on a magnetic stirrer while maintaining the reaction pH at a predetermined value by adding dilute HCl; this procedure is designated as "reduction reactions with pH control." The products formed were filtered, washed with deionized water unless otherwise specified, and allowed to dry in air. The products were then fired in air for 24 h at 300–900°C unless otherwise specified.

Ion-exchange reactions of the fired Na_xMnO_2 samples were carried out both at ambient temperature and at higher temperatures. The ambient temperature ion exchange was carried out by stirring the samples for 24 h with a 4-fold excess $LiCF_3SO_3$ solution in acetonitrile. The high-temperature ion exchange was carried out by refluxing the sample for 12 h with a 10-fold excess LiBr solution in hexanol at 180°C. Oxidative extraction of sodium from the fired Na_xMnO_2 samples was carried out by stirring for 24 h with a fivefold excess iodine solution in acetonitrile. The products formed after the ion-exchange and sodium extraction reactions were filtered, washed with acetonitrile, and dried.

The samples were characterized by X-ray powder diffraction. Lithium, sodium, and manganese contents were determined by atomic absorption spectroscopy. Oxygen contents were determined by a potentiometric redox titration employing vanadyl sulfate (16). Iodine content was determined by oxidizing I^- with hydrogen peroxide followed by extracting the iodine with CCl_4 and titrating with sodium thiosulfate (17). Surface area was evaluated by the BET method with a Qunatachrome Autosorb-1 instrument. Thermogravimetric analysis (TGA) data were collected with a Perkin-Elmer Series 7 instrument at a heating rate of 2°C/min in a flowing mixture of 80% N_2 and 20% O_2. Magnetic properties were evaluated with a SQUID magnetometer and an applied field of 1000 Oe. There were no significant differences between the zero-field-cooled and field-cooled data and the data presented later in this paper refer to field-cooled data.

3. RESULTS AND DISCUSSION

3.1. Reduction Reactions without pH Control

Wet chemical analysis of the products obtained by reducing 100 mL of 0.5 M $NaMnO_4 \cdot H_2O$ with 100 mL of various concentrations (0.05–3 M) of NaI without controlling the pH indicated a Na/Mn ratio of around 0.7 irrespective of the concentration of NaI. The final pH in these reactions after mixing the two reactants was found to be above 11. TGA data reveal that the as-prepared samples contain significant amount of water (<25 wt%), which is lost on heating at $T < 300$°C. Table 1 gives the compositions of the products obtained after firing at various temperatures the precipitate formed by reducing 100 mL of 0.5 M $NaMnO_4 \cdot H_2O$ with 100 mL of 0.5 M NaI. The analytical data show that the products fired at $T \leq 500$°C contain a small amount of iodine, which decreases with increasing firing temperature, and those fired at $T \geq 600$°C do not contain any iodine; the decrease in iodine content with increasing firing temperature was also confirmed by a continuous weight loss in TGA up to 600°C. The observed

TABLE 1
Wet Chemical Analysis and the Surface Area Data of Products Obtained by Reducing 100 mL of 0.5 M $NaMnO_4 \cdot H_2O$ with 100 mL of 0.5 M NaI

Firing temperature (°C)	Composition[a]	Surface area (m^2/g)	Magnetic susceptibility		Composition after	
			μ_{eff} (calc)	μ_{eff} (meas)	Ion exchange[b]	Sodium extraction
300	$Na_{0.71}MnO_{2.39}I_{0.098}$					
400	$Na_{0.71}MnO_{2.38}I_{0.028}$		3.793			
500	$Na_{0.70}MnO_{2.31}I_{0.026}$	59	3.956	3.940	$Li_{0.59}Na_{0.16}MnO_{2.33}I_{0.022}$ ($Li_2Mn_2O_4 + Na_{0.7}MnO_{2+\delta}$)	$Na_{0.63}MnO_{2.27}I_{0.036}$
600	$Na_{0.69}MnO_{2.29}$ $[Na_{0.60}Mn_{0.87}O_2]$	39	3.986	3.965	$Li_{0.60}Na_{0.14}MnO_{2.33}$ ($Li_2Mn_2O_4 + Na_{0.7}MnO_{2+\delta}$)	$Na_{0.64}MnO_{2.27}$
700	$Na_{0.68}MnO_{2.28}$ $[Na_{0.60}Mn_{0.88}O_2]$		3.997			
800	$Na_{0.68}MnO_{2.25}$ $[Na_{0.60}Mn_{0.89}O_2]$	9	4.059	3.959	($Li_2Mn_2O_4 + Na_{0.7}MnO_{2+\delta}$)	$Na_{0.64}MnO_{2.23}$
900	$Na_{0.67}MnO_{2.22}$ $[Na_{0.60}Mn_{0.90}O_2]$		4.110	4.016		

[a]Crystallographic compositions based on an oxygen content of 2.00 are given in square brackets.
[b]Phase identifications are given in parantheses; data correspond to ion-exchange reactions carried out at room temperature.

iodine content could be due to an inefficient removal by water washing of the reaction product I_2 formed during the reduction reaction. The removal of small amount (~ 0.03) of iodine for $T > 400°C$ is accompanied by a small decrease in Na content, which could be due to the elimination of iodine as NaI since NaI has a melting point of 660°C and volatilizes at $T > 400°C$. The analytical data also show that the samples have an oxygen content of >2 and the oxygen content decreases with increasing firing temperature due to a decrease in the oxidation state of manganese. However, density measurements of $Na_xMnO_{2+\delta}$ have shown that the excess δ oxygen atoms are accommodated by cation vacancies in the lattice rather than as interstitial oxygen atoms (18). Accordingly, the crystallographic compositions based on an oxygen content of 2.00 are given in square brackets in Table 1 for the samples that do not contain iodine and are fired at $T > 600°C$.

Figure 1 shows the X-ray diffraction patterns of the sample obtained by reducing 100 mL of 0.5 M $NaMnO_4 \cdot H_2O$ with 100 mL of 0.5 M NaI (sample in Table 1). The as prepared sample does not show any discernible reflections (Fig. 1a). The sample fired at 600°C show reflections (Fig. 1c) corresponding to hexagonal $Na_{0.7}MnO_{2+\delta}$, ($0.05 < \delta < 0.3$) that has a layer structure designated as $P2$ structure (8, 9). Further firing of this hexagonal $Na_{0.7}MnO_{2+\delta}$ in N_2 atmosphere at 600°C (Fig. 1f) gives orthorhombic $Na_{0.7}MnO_{2+\delta}$ ($\delta < 0.05$) having a distorted $P2$ structure (8, 9). On the other hand, the sample fired at 500°C (Fig. 1b), although showing resemblance to the hexagonal $Na_{0.7}MnO_{2+\delta}$ in Fig. 1c, exhibits poorly defined peaks excepting the (00l) reflections. The poorly defined, broad (hkl) reflections could be due to the cation disorder arising from a high concentration of cation vacancies, which in turn results from a high oxygen content ($\delta > 0.3$).

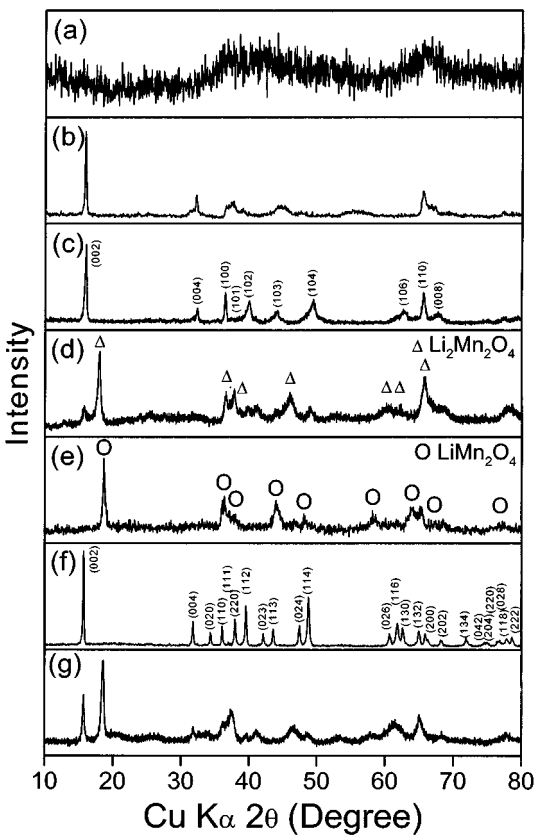

FIG. 1. X-ray powder diffraction patterns of the samples obtained by reducing 100 mL of 0.5 M $NaMnO_4 \cdot H_2O$ with 100 mL of 0.5 M NaI (sample in Table 1): (a) as-prepared sample, (b) after heating at 500°C, (c) after heating at 600°C, (d) after ion-exchanging sample c with $LiCF_3SO_3$ in acetonitrile, (e) after ion-exchanging sample c with LiBr in hexanol at 180°C, (f) after heating sample c in N_2 atmosphere at 600°C, and (g) after ion-exchanging sample f with LiBr in hexanol at 180°C.

It should be noted that the hexagonal $Na_{0.7}MnO_{2+\delta}$ ($0.05 < \delta < 0.3$) could be obtained only by using an oxygen atmosphere in the case of conventional solid-state reaction between sodium carbonate and manganese oxide, which is consistent with the literature data (8, 9). The solid-state reaction in air gives impurity phases at 600°C due to incomplete reaction and a mixture of $Na_{0.7}MnO_{2+\delta}$ and tunnel $Na_{0.5}MnO_{2+\delta}$ (see below) at 800°C. Interestingly, with the solution-based procedure described in this study, hexagonal $Na_{0.7}MnO_{2+\delta}$ ($0.05 < \delta < 0.3$) without impurity phases, could be obtained in ambient atmosphere (air) at 600–800°C.

Table 1 also gives the surface area of the products after firing at various temperatures. The surface area decreases from 59 to 9 m^2/g as the firing temperature increases from 500 to 800°C due to a coarsening of the grains. Figure 2 gives the magnetic data of the samples given in Table 1. All the samples are paramagnetic above about 150 K. The sample fired at 500°C shows a broad antiferromagnetic

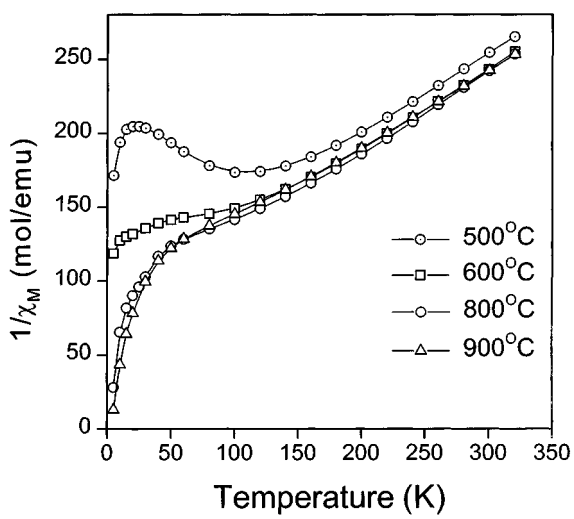

FIG. 2. Variation of inverse molar magnetic susceptibility of $Na_{0.7}MnO_{2+\delta}$ (sample in Table 1) with temperature.

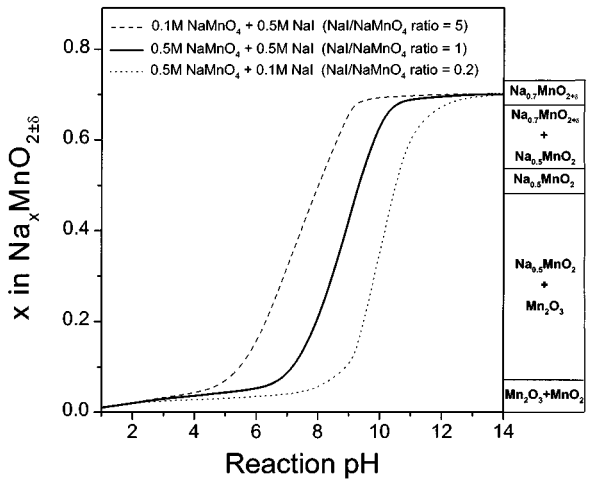

FIG. 3. Variation of sodium content x in the reaction product $Na_xMnO_{2+\delta}$ with reaction pH for various concentrations of the reactants (50 mL each). The analysis of the phases formed after firing the products at 600°C is also indicated for various values of x.

ordering around 120 K followed by a possible weak ferromagnetic ordering around 20 K. The antiferromagnetic ordering is suppressed as the firing temperature increases and the samples fired at $T \geq 800$°C show only the weak ferromagnetic component at $T < 50$ K. Table 1 compares the measured magnetic moments in the temperature range 200–300 K with that calculated for high-spin $Mn^{3+/4+}$ ions. The measured values are in close agreement with the calculated values. The magnetic moment increases with increasing firing temperature due to an increase in the number of unpaired electrons arising from a decrease in the oxidation state of manganese.

3.2. Reduction Reactions with pH Control

Since the reduction reactions described in the previous section without pH control gave invariably a Na/Mn ratio of around 0.7, we turned to pursue the reactions as a function of pH with an aim to obtain products with various Na/Mn ratios. Accordingly, 50 mL of 0.1 and 0.5 M $NaMnO_4 \cdot H_2O$ was reduced with 50 mL of 0.1 and 0.5 M NaI at a specified pH value. Figure 3 gives the variation of Na/Mn ratio (x value in $Na_xMnO_{2+\delta}$) in the reduction product with reaction pH. The amount of Na is negligible or very small in the reduction products synthesized under acidic conditions with pH < 5. For the range 5 < pH < 12, the Na content increases rapidly with increasing pH and reaches a maximum value of around 0.7. The curves in Fig. 3 show a dependence on the concentration of the reactants and the curves are shifted to higher pH values as the ratio of $NaI/NaMnO_4 \cdot H_2O$ decreases. The data in Fig. 3 explain why products with a Na/Mn ratio of around 0.7 ($x \approx 0.7$) were obtained invariably with all concentrations of NaI for the reactions described in the previous section (3.1) without pH control, in which the reaction pH was found to be above 11. It should be noted that water also participates in the reduction of permanganate ion depending on the pH in addition to the iodide ion. As a result, the products obtained are not simply due to a stoichiometric reaction between permanganate and iodide ions. Additionally, reduction of permanganate was found to be incomplete with lower concentrations of NaI (0.1 M) in Fig. 3 as indicated by the color of the filtrate.

Figure 3 also gives the phase analysis data for various values of Na content x. The phase analysis was carried out by X-ray diffraction after firing the reduction products at 600°C in air. Binary manganese oxides are formed for low values of $x < 0.07$. Sodium manganese oxide with a tunnel structure is formed for $x = 0.5 \pm 0.02$, and with a hexagonal layer structure ($P2$ structure discussed in the previous section 3.1) is formed for $x = 0.7 \pm 0.03$. Two phase regions are found for other x values as indicated in Fig. 3.

Table 2 gives the compositions of the products obtained after firing at various temperatures the precipitate formed

TABLE 2
Wet Chemical Analysis and Surface Area Data of Products Obtained by Reducing 50 mL of 0.5 M $NaMnO_4 \cdot H_2O$ with 50 mL of 0.5 M NaI at a Controlled pH Value of 9.3

Firing temperature (°C)	Composition[a]	Surface area (m^2/g)	Magnetic susceptibility		Composition after	
			μ_{eff} (calc)	μ_{eff} (meas)	Ion exchange[b]	Sodium extraction
300	$Na_{0.51}MnO_{2.16}I_{0.031}$		4.027			
500	$Na_{0.5}MnO_{2.15}I_{0.009}$	48	4.079	3.836	$Na_{0.06}Li_{0.46}MnO_{2.16}I_{0.006}$	$Na_{0.37}MnO_{2.13}I_{0.021}$
600	$Na_{0.5}MnO_{2.06}$ $[Na_{0.485}Mn_{0.97}O_2]$	21	4.264		$Na_{0.16}Li_{0.38}MnO_{2.08}$	$Na_{0.35}MnO_{2.05}$
800	$Na_{0.49}MnO_{2.00}$ $[Na_{0.49}MnO_2]$	6	4.387	4.099	$Na_{0.16}Li_{0.37}MnO_{2.01}$	$Na_{0.35}MnO_{2.00}$

[a]Crystallographic compositions based on an oxygen content of 2.00 are given in square brackets.
[b]Data correspond to ion-exchange reactions carried out at room temperature.

by reducing 50 mL of 0.5 M $NaMnO_4 \cdot H_2O$ with 50 mL of 0.5 M NaI at a controlled pH of 9.3. As found in Table 1, the products fired at $T \leq 500°C$ contain a small amount of iodine, which decreases with increasing firing temperature, and those fired at $T \geq 600°C$ do not contain any iodine. The iodine content in the samples was also found to depend on the reaction pH. The iodine content was found to decrease as the reaction pH decreases from 11 to 7 and then to increase slightly as the pH decreases from 7 to 1. Thus the samples synthesized close to neutral pH had the least amount of iodine content. The oxygen content in the products decreases with increasing firing temperature due to a decrease in the oxidation state of manganese. As in Table 1, the crystallographic compositions based on an oxygen content of 2.00 are given in square brackets in Table 2 for the samples that do not contain iodine. However, the oxygen nonstoichiometry in Table 2 is to a lesser degree than that in Table 1 and the sample fired at 800°C has an oxygen content of 2.00 without cation vacancies.

Figure 4 shows the X-ray diffraction patterns of the sample in Table 2 with a Na/Mn ratio of around 0.5. The as-prepared sample does not show any discernible reflections (Fig. 4a). The sample fired at 500°C (Fig. 4b) shows three broad reflections, which could be indexed on a hexagonal layer structure with $a = 2.839$ Å and an undefined c parameter (19). The three reflections centered around approximately $2\theta = 16°$, 37°, and 66° refer, respectively, to (00l), (100), and (110) reflections. Since there is no observable (hkl) reflection, the c parameter could not be defined and the material could thus be turbostratic. For example, the c parameter could be 5.56 Å ($l = 1$), 11.12 Å ($l = 2$), 16.68 Å ($l = 3$) or multiples of 5.56 Å depending on the value of l for the first reflection centered around $2\theta = 16°$. Although the X-ray pattern in Fig. 4b shows some resemblance to that reported in the literature (20) for a close composition $Na_{0.45}MnO_{2+\delta}$ that was obtained by washing with water a sol–gel synthesized $Na_{0.7}MnO_{2.14} \cdot 0.3NaOH$, it could not be established unambiguously that the two samples are identical due to poor crystallinity and a fewer number of reflections. The sample fired at 600°C (Fig. 4e), on the other hand, show several sharp reflections, which correspond to the orthorhombic $Na_{0.44}MnO_2$ (8, 9) that has a tunnel structure isostructural with $Na_4Mn_4Ti_5O_{18}$ (21). The tunnel structure is maintained on raising the firing temperature further to 800°C. The 600 and 800°C samples have a lattice parameters of, respectively, $a = 9.091$ (1), $b = 26.422$ (6), and $c = 2.825(1)$ and $a = 9.076(1)$, $b = 26.445(6)$, and $c = 2.8232(5)$, which are in close agreement with that reported in the literature for $Na_{0.44}MnO_2$ (8).

Recently, the tunnel $Na_{0.44}MnO_2$ has drawn considerable attention as a cathode material in lithium cells (10, 11, 22, 23) as it does not transform to the spinel-like phases during the electrochemical charge–discharge cycling while most other nonspinel manganese oxides tend to transform to spinel-like phases. However, the $Na_{0.44}MnO_2$ composition reported in the literature is invariably contaminated with Mn_2O_3 impurity phase. Interestingly, the 600°C sample in Fig. 4 with a Na/Mn ratio of 0.5 consists of single phase tunnel material without Mn_2O_3 or other impurities as indicated by Rietveld analysis. This observation immediately raises the question that the tunnel structure may be formed for $x = 0.5$ rather than for $x = 0.44$ in Na_xMnO_2. In order to clarify this issue, we have carried out solid-state reactions at 800°C in air with various ratios of Na_2CO_3 and Mn_2O_3. Since there is a possibility of volatilization of sodium at higher temperatures, the sodium and manganese contents of the products obtained by solid-state reaction were also analyzed by atomic absorption spectroscopy. The analytical data reveal that there is no loss of

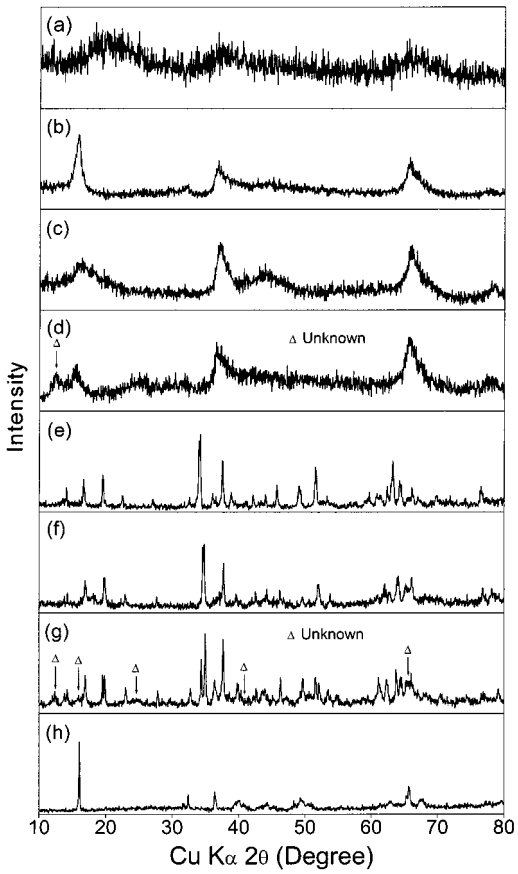

FIG. 4. X-ray powder diffraction patterns of the samples obtained by reducing 50 mL of 0.5 M $NaMnO_4 \cdot H_2O$ with 50 mL of 0.5 M NaI at a controlled pH of 9.3 (sample in Table 2): (a) as-prepared sample, (b) after heating at 500°C (layer structure), (c) after ion exchanging sample b with $LiCF_3SO_3$ in acetonitrile, (d) after extracting sodium from sample b with iodine in acetonitrile, (e) after heating at 600°C (tunnel structure), (f) after ion exchanging sample e with $LiCF_3SO_3$ in acetonitrile, (g) after extracting sodium from sample e with iodine in acetonitrile, and (h) after washing the reaction product with acetonitrile and heating at 600°C ($P2$ layer structure similar to that found for hexagonal $Na_{0.7}MnO_{2+\delta}$).

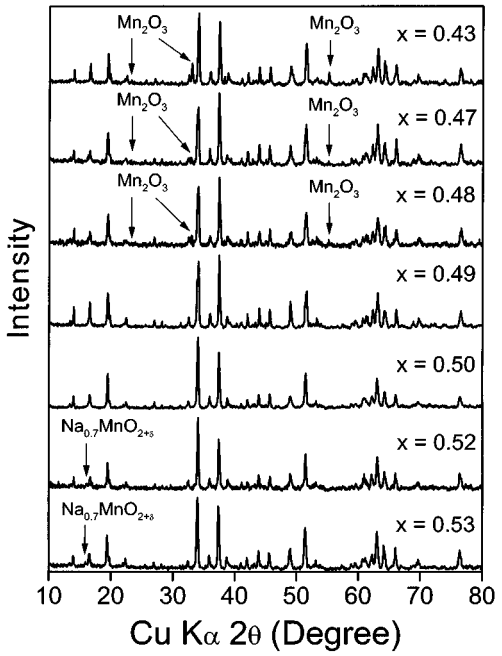

FIG. 5. X-ray diffraction patterns of Na_xMnO_2 that were obtained by firing various ratios of Na_2CO_3 and Mn_2O_3 at 800°C in air. The unmarked reflections correspond to the tunnel structure. The reflections corresponding to Mn_2O_3 and $Na_{0.7}MnO_{2+\delta}$ impurities are indicated by arrows.

sodium. The X-ray patterns of the samples obtained by solid-state reaction are given in Fig. 5 (24). The data clearly reveal that the tunnel structure is formed for $x = 0.5$ in Na_xMnO_2 and not for $x = 0.44$. Compositions with $x < 0.5$ show Mn_2O_3 impurity while those with $x > 0.5$ show $Na_{0.7}MnO_{2+\delta}$ impurity. Since the samples fired at 800°C do not contain excess oxygen ($\delta = 0$) or cation vacancies (Table 2), the results unambiguously demonstrate that the tunnel structure is formed for $x = 0.5$ in Na_xMnO_2.

The formation of the tunnel structure for $x = 0.5$ in Na_xMnO_2 rather than for the expected value of $x = 0.44$ in analogy with $Na_4Mn_4Ti_5O_{18}$ could be understood by considering the crystal structure (Fig. 6). The structure of $Na_4Mn_4Ti_5O_{18}$ consists of MnO_5 square pyramids and MnO_6 octahedra, which are connected together by sharing edges and corners to give two types of tunnels: one large S-shaped tunnel and two pentagonal tunnels per unit cell. While each S-shaped tunnel contains four Na sites, each pentagonal tunnel contains one Na site. In $Na_4Mn_4Ti_5O_{18}$ ($x = 0.44$), all the Na sites in the pentagonal tunnels (corresponding to $x = 0.22$) and 50% of the Na sites in the S-shaped tunnels (corresponding to $x = 0.22$) are occupied. In $Na_{0.5}MnO_2$ with $x = 0.5$, all the Na sites in the pentagonal tunnels (corresponding to $x = 0.22$) and 62.5% of the Na sites in the S-shaped tunnels (corresponding to $x = 0.28$) will be occupied.

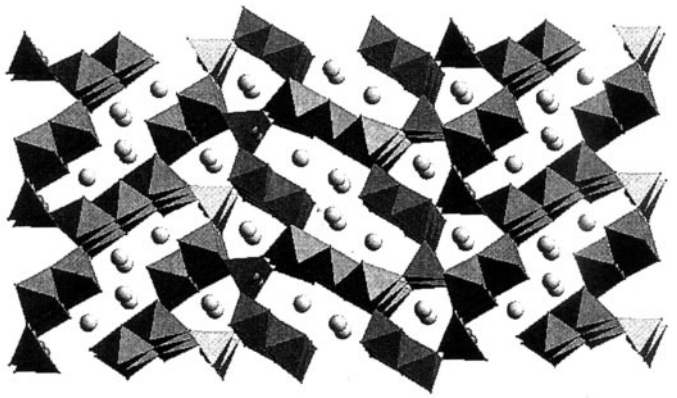

FIG. 6. Crystal structure of tunnel $Na_{0.5}MnO_2$ (previously thought to be $Na_{0.44}MnO_2$ in the literature) isostructural with $Na_4Mn_4Ti_5O_{18}$.

Table 2 also gives the surface area of the products after firing at various temperatures. The surface area decreases from 48 to 6 m^2/g as the firing temperature increases from 500 to 800°C. The magnetic data of the $Na_{0.5}MnO_{2+\delta}$ samples are given in Fig. 7 and Table 2. While the tunnel sample obtained after firing at 800°C shows an antiferromagnetic order around 30 K, the layered sample obtained after firing at 500°C shows a slight increase in susceptibility at lower temperatures $T < 40$ K. The measured magnetic moments in the temperature range 200–300 K are in close agreement with the calculated values. The magnetic moment increases with increasing firing temperature due to decreasing oxidation state of manganese.

3.3. *Effect of Washing on the Reduction Products*

Since I_2 is formed as one of the reaction products and its solubility in water is very low, the effect of washing the

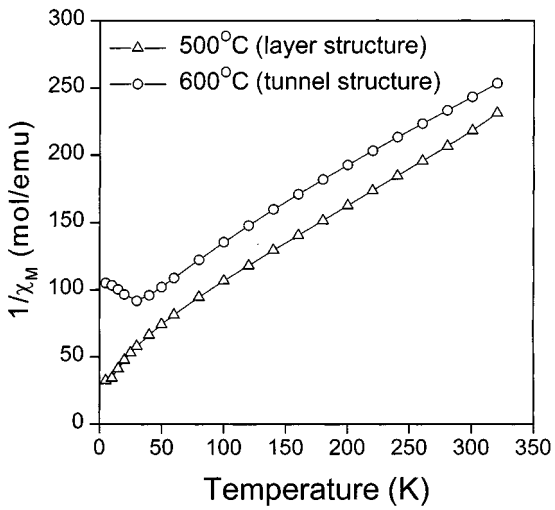

FIG. 7. Variation of inverse molar magnetic susceptibility of $Na_{0.5}MnO_{2+\delta}$ (sample in Table 1) with temperature.

reduction products with other solvents such as acetonitrile, acetone and ethanol was investigated. While iodine is highly soluble in acetonitrile and acetone, it is only slightly soluble in ethanol. Washing of the reduction products obtained by reducing 50 mL of 0.5 M $NaMnO_4 \cdot H_2O$ with 50 mL of 0.5 M NaI at a controlled pH of 9.3 (sample in Table 2) with water or ethanol followed by firing at 600°C gave $Na_{0.5}MnO_{2+\delta}$ ($\delta \leq 0.06$) having the tunnel structure as seen in Fig. 4e. On the other hand, washing of the products with acetonitrile or acetone followed by firing at the same temperature of 600°C gave $Na_{0.5}MnO_{2+\delta}$ ($\delta > 0.1$) having a hexagonal layer structure (Fig. 4h) similar to that of $Na_{0.7}MnO_{2+\delta}$ (*P*2 layer structure). The higher oxygen content in the acetonitrile-washed product seems to favor the layer structure instead of the expected tunnel structure. This metastable layer structure was found to be maintained remarkably up to a firing temperature of 800°C. For firing temperatures $T \geq 900$°C, the tunnel phase begins to appear. The washing with different solvents thus appears to affect the reaction kinetics and thereby influence the oxygen content and the crystal chemistry of the product. Although washing with acetonitrile removes completely the reaction product iodine and thereby avoids a possible decrease in Na content on firing at $T > 400$°C due to the removal of iodine as NaI, the sodium contents were found to be similar ($x = 0.5 \pm 0.02$) in the water-washed and acetonitrile-washed products after firing at 600°C. Thus the differences observed in the crystal chemistry are not due to differences in Na contents.

3.4. Ion Exchange and Sodium Extraction Reactions

Due to a widespread interest in manganese oxides as cathode hosts in lithium cells, both ion-exchange reactions with lithium salts and sodium-extraction reactions with iodine of the products synthesized were investigated. The compositions of the products obtained after the ion-exchange and sodium-extraction reactions are given in Tables 1 and 2. The X-ray diffraction patterns of the products are given in Figs. 1 and 4.

With the $Na_{0.7}MnO_{2+\delta}$ composition, the hexagonal form ($\delta \approx 0.3$) with undistorted *P*2 structure and cation vacancies (Figs. 1c, 1d, and 1e) undergoes ion exchange more readily than the orthorhombic form ($\delta < 0.05$) with distorted *P*2 structure (Figs. 1f and 1g). With the hexagonal form, the ion exchange occurs to a greater degree at higher temperatures than at ambient temperature (Figs. 1d and 1e). More importantly, the ion-exchange reactions of the hexagonal form leads to the formation of the spinel $LiMn_2O_4$ (Fig. 1e) or lithiated spinel $Li_2Mn_2O_4$ (Fig. 1d), indicating the instability of the hexagonal form. On the other hand, the distorted orthorhombic form (Fig. 1f) is quite stable during the ion exchange reaction without transforming to the spinel-type phases (Fig. 1g), as indicated by a careful analysis and comparison of the intensity of the reflections in Figs. 1c–1g. The stability of the orthorhombic form is consistent with that recently found with the layered $Na_{0.67}[Li_{0.17}Mn_{0.83}]O_2$ that has the *P*2 structure without cation vacancies (25). It is remarkable that the *P*2 structure with no or little cation vacancies is quite stable while most manganese oxides with close-packed structures tend to transform to spinel-like phases. The distorted *P*2 structure thus has the potential to emerge as a candidate for lithium-ion cells (25, 26). We believe that the instability of the hexagonal form during ion-exchange reactions is due to the presence of cation vacancies arising from a high oxygen content. The cation vacancies seem to promote the migration of the Li^+ ions into the manganese layer and thereby favor the formation of spinel phases. However, only a small amount of sodium could be extracted by oxidation with iodine from both the forms (Table 1).

With the $Na_{0.5}MnO_{2+\delta}$ composition, the layer structure formed at 500°C undergoes a larger degree of ion-exchange than the tunnel structure (Table 2). The smaller degree of ion exchange in the latter is consistent with the difficulty of removal of Na^+ ions from the smaller pentagonal tunnels as found by Doeff *et al.* (11). Ion exchange under more drastic conditions (270°C) with eutectic mixtures is required to exchange all the Na^+ by Li^+ in the tunnel structure (23). On the other hand, both the structures undergo small but nearly the same degree of sodium extraction (0.14 ± 0.01 Na per $Na_{0.5}MnO_{2+\delta}$ formula) with iodine. While no impurity phases are formed during the ion exchange reactions (Figs. 4c and 4f), unknown impurity phases are formed during the sodium extraction reactions (Figs. 4d and 4g), as indicated by extra reflections and Rietveld analysis. Although some of the extra reflections seem to correspond to $Na_{0.25}MnO_2$, it could not be established unambiguously due to the poor crystallinity in Fig. 4d and possible overlap of peaks in Fig. 1g. More importantly, the tunnel phase does not transform to the spinel-like phases during ion exchange or sodium extraction as has been found before by Doeff *et al.* (10, 11, 22).

4. CONCLUSIONS

$Na_xMnO_{2+\delta}$ oxides have been synthesized by reducing sodium permanganate with sodium iodide in aqueous solutions followed by firing the reduction products at higher temperatures. The sodium content, oxygen content, and crystal chemistry of the products are influenced by the reaction pH, solvents used for washing the products, and the firing temperature. $Na_{0.7}MnO_{2+\delta}$ crystallizing in a hexagonal *P*2 structure ($\delta \approx 0.3$) and in a distorted orthorhombic *P*2 structure ($\delta \approx 0$) and $Na_{0.5}MnO_{2+\delta}$ crystallizing in two metastable layer structures and in a thermodynamically stable tunnel structure have been obtained. Both the orthorhombic $Na_{0.7}MnO_{2+\delta}$ ($\delta \approx 0$) and the tunnel

$Na_{0.5}MnO_{2+\delta}$ are stable to ion-exchange reactions with lithium salts, while the hexagonal $Na_{0.7}MnO_{2+\delta}$ ($\delta \approx 0.3$) is unstable to ion-exchange reactions forming spinel-like phases due to the migration of manganese ions promoted by the presence of cation vacancies. This observation may help in designing and developing structurally stable manganese oxide cathode hosts for lithium-ion batteries. Additionally, while it is difficult to synthesize $Na_{0.7}MnO_{2+\delta}$ by conventional solid-state reactions in air, the solution-based approach described in this paper accesses readily $Na_{0.7}MnO_{2+\delta}$ in ambient air over a range of temperatures $500 \leq T \leq 900^{\circ}C$.

ACKNOWLEDGMENT

This work was supported by the Welch Foundation Grant F-1254 and Texas Advanced Technology Program Grant 003658-0488-1999.

REFERENCES

1. P. Strobel and J. Charenton, *Rev. Chim. Miner.* **23,** 125 (1986).
2. M. M. Thackeray, *Prog. Solid State Chem.* **25,** 1 (1997).
3. R. Von Helmolt, J. Wecker, B. Holzapfelh, L. Schultz, and K. Samwer, *Phys. Rev. Lett.* **71,** 2331 (1993).
4. R. Huber, K. V. Kordesch, A. Kozawa, and D. B. Wood, *in* "Batteries" (K. V. Kordesch, Ed.), Vol. 1. Dekker, New York, 1974.
5. H. J. M. Bouwmeester and A. J. Burggraaf, *in* "The CRC Handbook of Solid State Electrochemistry" (P. J. Gellings and H. J. M. Bouwmeester, Eds.), p. 481. CRC Press, New York, 1997.
6. C. G. Vayenas, S. I. Bebelis, I. V. Yentekakis, and S. N. Neophytides, *in* "The CRC Handbook of Solid State Electrochemistry" (P. J. Gellings and H. J. M. Bouwmeester, Eds.), p. 445. CRC Press, New York, 1997.
7. A. Manthiram and J. Kim, *Chem. Mater.* **10,** 2895 (1998).
8. J. Parant, R. Olazcuaga, M. Devalette, C. Fouassier, and P. Hagenmuller, *J. Solid State Chem.* **3,** 1 (1971).
9. A. Mendiboure, C. Delmas, and P. Hagenmuller, *J. Solid State Chem.* **57,** 323 (1985).
10. M. M. Doeff, M. Y. Peng, Y. Ma, and L. C. De Jonghe, *J. Electrochem. Soc.* **141,** L145 (1994).
11. M. M. Doeff, T. J. Richardson, and L. De Kepley, *J. Electrochem. Soc.* **143,** 2507 (1996).
12. S. Ching, D. J. Petrovay, M. L. Jorgensen, and S. L. Suib, *Inorg. Chem.* **36,** 883 (1997).
13. P. Le Goff, N. Baffier, S. Bach, and J. P. Pereira-Ramos, *Mater. Res. Bull.* **31,** 63 (1996).
14. Y. F. Shen, R. P. Zerger, R. N. DeGuzman, S. L. Suib, L. McCurdy, D. I. Potter, and C. L. O'Young, *Science* **260,** 511 (1993).
15. Q. Feng, H. Kanoh, Y. Miyai, and K. Ooi, *Chem. Mater.* **7,** 1722 (1995).
16. C. Tsang and A. Manthiram, *Solid State Ionics* **89,** 305 (1996).
17. J. Kim and A. Manthiram, *Nature* **390,** 265 (1997).
18. C. Delmas and C. Fouassier, *Z. Anorg. Allg. Chem.* **420,** 184 (1976).
19. Y. U. Jeong and A. Manthiram, *Electrochem. Solid State Lett.* **2,** 421 (1999).
20. P. Le Goff, N. Baffier, S. Bach, J. P. Pereira-Ramos, and R. Messina, *Solid State Ionics* **61,** 1 (1971).
21. W. G. Mumme, *Acta Crystallogr. B* **24,** 1114 (1968).
22. M. M. Doeff, L. Ding, and L. C. De Jonghe, *Mater. Res. Soc. Symp. Proc.* **393,** 107 (1995).
23. A. R. Armstrong, H. Huang, R. A. Jennings, and P. G. Bruce, *J. Mater. Chem.* **8,** 255 (1998).
24. A. Manthiram and Y. U. Jeong, "Electrochemical Society Proceedings" (G. A. Nazri, T. Ohzuku, and M. M. Thackeray, Eds.), Vol. 99–24, p. 29. The Electrochemical Society, Pennington, NJ, 2000.
25. J. M. Paulsen, C. L. Thomas, and J. R. Dahn, *J. Electrochem. Soc.* **146,** 3560 (1999).
26. J. M. Paulsen and J. R. Dahn, *Solid State Ionics* **126,** 3 (1999).